



ATLAS Simulation Studies Related to the Design of the Inner Tracker for the HL-LHC

Omar F. Sosa Rodríguez, Deutsches Elektronen-Synchrotron, Germany

September 7, 2012

Abstract

The phase-II upgrade of the LHC is escheduled for 2022 and is expected to provide a high luminosity scenario, with many possibilities for physics but very challenging experimentally. An upgrade of the ATLAS detector is required if the best use is to be made of these future conditions. The proposal is to build an all-silicon tracker with pixel and microstrip technology. The layout for the new inner detector is presented here as well as the simulation studies that have been carried out for different pixel geometries of the endcap pixel detector.

Contents

1	Introduction	3
2	The ATLAS Experiment	4
2.1	The ATLAS Inner Detector	4
3	Letter of Intent Layout	6
4	Simulation Description	7
5	Results	10
6	Conclusions	11

1 Introduction

The Large Hadron Collider (LHC) is currently the most powerful particles accelerator, it is located at the European laboratory of physics, CERN, in the frontier of France and Switzerland. It is a proton-proton collider and it is designed to operate with the followings parameters:

Parameter	Value
Luminosity	$L = 5 \times 10^{34} cm^{-2} s^{-1}$
Center of mass energy	$\sqrt{s} = 14 TeV$
Pile-up	140 pp interactions

Table 1: Design parameter of the LHC

However, this is not the current situation. The LHC must undergo a series of upgrades in order to reach the expected parameters. The upgrade for which these parameters will start to operate is planned for 2022-23 and it's called the *Phase-II Upgrade*. Due to the high luminosity conditions, the accelerator will be called HL-LHC, which stands for High Luminosity - Large Hadron Collider (in some papers it is referred as SLHC, for Super LHC). The following table shows a comparison between the current parameters of the LHC and the parameters expected for the HL-LHC:

Parameter	LHC (2012)	HL-LHC (2022)
Luminosity	$L = 7 \times 10^{33} cm^{-2} s^{-1}$	$L = 5 \times 10^{34} cm^{-2} s^{-1}$
Center of mass energy	$\sqrt{s} = 8 TeV$	$\sqrt{s} = 14 TeV$
Pile-up	25 pp interactions	140 pp interactions

Table 2: Comparison between LHC and HL-LHC

There are many motivations for upgrading the LHC to the HL-LHC. Some of them are

- Study Standard Model physics with more precision,
- Supersymmetry,
- Extra dimensions,
- Higgs boson physics,

and more. Precise experiments in these topics require high luminosity conditions.

However, this scenario is very challenging experimentally. The current detectors of the ATLAS experiment (which will be explained below) are not suitable for operation in such

an environment, mainly because of the radiation damage that will have been sustained for when the phase-II upgrade takes place. Among other reasons are the insufficient granularity that the current inner detector poses to distinguish tracks in a pile-up scenario of 140 pp interactions per bunch crossing, and the fact that the TRT system is not appropriate to operate in a high luminosity environment. All these points will be explained in the following section.

2 The ATLAS Experiment

ATLAS is a particle physics experiment at the Large Hadron Collider at CERN. The ATLAS detector consists, essentially, of four components:

- **Inner Detector:** Measures the momentum of each charged particle.
- **Calorimeter:** Measures the energies carried by the particles.
- **Muon Spectrometer:** Identifies and measures the momenta of muons.
- **Magnet System:** Bends charged particles for momentum measurement.

In this paper we'll focus only on the inner detector and how it works.

2.1 The ATLAS Inner Detector

The ATLAS inner detector (ID) currently consists of three subsystems: Pixel detector, Semiconductor Tracker (SCT), and the Transition Radiation Tracker. How these components are setup is shown in Figure 1. The inner detector is used for track and vertex reconstruction. All charged particles that pass through the detector leave hits (energy deposits) that the detector electronics uses to reconstruct the tracks and to obtain other important information about the event. For this reason the ID, and more specifically the pixel detector, requires high resolution, otherwise it won't be capable of distinguish correctly one track from another. Due to the high amount of radiation for $|\eta| > 2.5$, the detectors acceptance is up to this value¹.

Since I've been working only on the pixel detector I will not explain how the SCT or the TRT is formed, this information can be found in ??.

¹Recall that $\eta = -\ln[\tan \frac{\theta}{2}]$ and θ is the usual spherical coordinates angle, taking the z axis as the beam line.

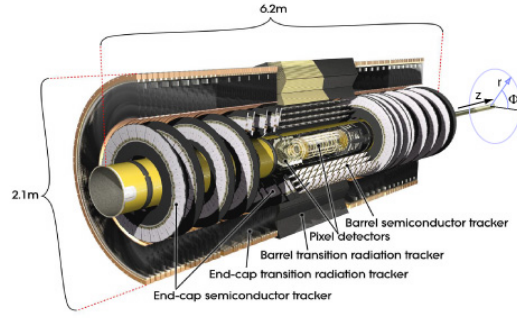


Figure 1: Inner detector setup

Pixel detector The ATLAS Pixel Detector is the center of this work. It provides a very high granularity, high precision set of measurements as close to the interaction point as possible. The system provides three precision measurements and mostly determines the impact parameter resolution and the ability of the Inner Detector to find short lived particles such as B-Hadrons. The current system layout consists of three barrels layers at average radii of $\sim 5cm$, $9cm$, and $12cm$, and three disks on each side (endcap), between radii of 9 and $15cm$. Each barrel layer and each endcap disk is made out of modules, using a total of 1456 modules for the barrel and 288 for the endcap. Each module is 62.4 mm long and 21.4 mm wide, with 46080 pixel elements read out by 16 chips, each serving an array of 18 by 160 pixels. The 80 million pixels cover an area of $1.7 m^2$. The readout chips must withstand over 300kGy of ionising radiation and over 5×10^{14} neutrons per cm^2 over ten years of operation. The modules are overlapped on the support structure to give hermetic coverage. The thickness of each layer is expected to be about 2.5 of a radiation length at normal incidence. Typically three pixel layers are crossed by each track.

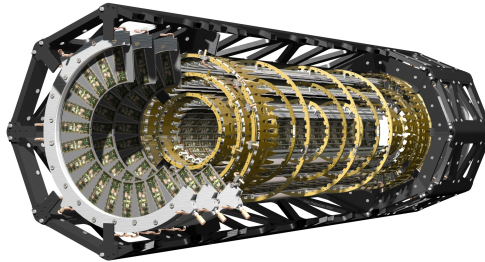


Figure 2: ATLAS Pixel detector

Within ten years the amount of radiation damage in the pixel detector obligates to make a replacement regardless of the luminosity conditions. However this replacement will be taken as an opportunity to upgrade the ATLAS inner detector to an appropriate system for the high luminosity of the phase-II upgrade. The idea is to replace the current

detector for an all-silicon system using only pixel and microstrip technology, no TRT, building this way a detector that is more resistant to radiation. This layout proposal is detailed in the next section and it's called 'Letter of Intent' (LoI) layout.

3 Letter of Intent Layout

The Inner Tracker upgrade (ITk) layout 'Letter of Intent' was designed to adress shortcomings in the 'Utopia' laoyout ??, used before for ITk studies. As mentioned before, this will be an all-silicon tracker, composed of two subsystems: The pixel detector, using pixel sensor technology; and the SCT, using silicon microstrips. Figure 3 shows how the layers of this systems are arranged.

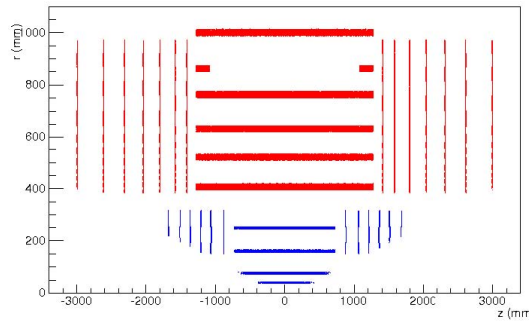


Figure 3: Sensitive layers in the LoI layout (r-z view), Pixel and Strip systems are shown in blue and red respectively

Strip System This is the outer system of the ID and consists of five barrel layers with radii from 405 - 1000 mm, and seven endcap disks at z -positions between ± 1415 mm and ± 3000 mm. There are also two 'stub cylinders' at either end of the barrel between the fourth and fifth layers, these are to provide coverage in an η region which otherwise has a hits deficiency.

For the three inner layers the strips length is 23.82 mm, whereas the two remaining layers use strips of length 47.64 mm (the same as the 'stub cylinders'). It's worth saying that the strip sensors are double sided, therefore each sensor provides two hits for the reconstruction of the tracks. In the endcap, the strip length ranges from 8.1 mm (for the innermost region) to 58.3 mm.

Pixel System The LoI pixel system is composed of four barrel layers, with radii from 39 mm for the inner layer to 250 mm for the outer layer, and six endcap disks at z -positions from ± 877 mm for the innermost disk to ± 1675 mm for the outermost. Each

endcap disk is made out of three different types of rings, which in turn are divided in modules (and so are the barrel layers). Modules are subdivided in sensors, and sensors are formed by many pixels. Figure 4 illustrates this arrangement. The pixels size for the 2 innermost barrel layers is $25 \times 150 \mu m^2$, while the two remaining layers have pixels of size $50 \times 250 \mu m^2$. The size of the pixels in the endcap disks is still to be decided, there are three proposals so far:

1. Rectangular $50 \times 250 \mu m^2$ pixels.
2. Squared $50 \times 50 \mu m^2$ pixels.
3. Squared $100 \times 100 \mu m^2$ pixels.

The objective of this work is to run simulations with these three different proposals in order to decide which pixel size is the best option for the endcap.

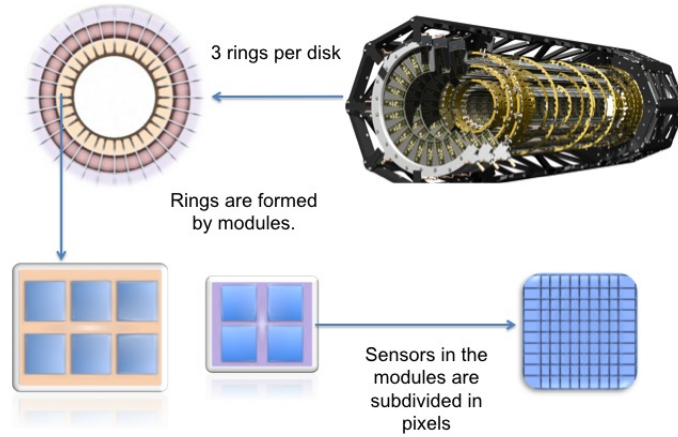


Figure 4: Diagram to illustrate how the pixel endcap is composed: Disk→Ring→Module→Sensor→Pixel. Proportions in the image are not correct.

4 Simulation Description

The simulation studies are carried out within the ATLAS Athena framework, using mostly a Monte Carlo production. The Athena framework is an enhanced version of the Gaudi framework, originally developed by the LHCb experiment, but it's now commonly used in the ATLAS experiment. Athena has a component based architecture designed for a wide range of physics data processing applications. This architecture allows flexibility in developing a range of shared components and, when necessary, components that

are specific to a particular experiment.

The design of the detector is included in the GeoModel package, this includes sensors, modules, support structures, service materials, etc. A complete model of the detector is achieved when GeoModel interfaces with the simulation toolkit Geant4.

The simulation data flow has three basic steps:

1. **Simulation** This step uses the Monte Carlo simulated event to distribute energy deposits (Hits) in the simulated detector.
2. **Digitization** Takes the simulated energy deposits, and models the detector response and stores the information in form of Raw Data Objects (RDO's). This considers the electronics that are being used.
3. **Reconstruction** The RDO's are used to reconstruct the simulated event, and to create particle tracks from the space point information

Figure 5 illustrates these steps.

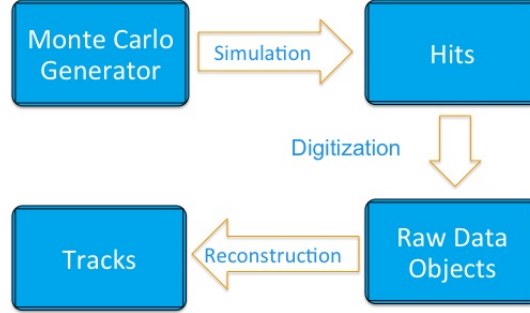


Figure 5: Simulation data flow

After the simulation, the reconstructed tracks have to be compared with the Monte Carlo truth objects (this is the information of the original characteristics of the particles that were created) in order to evaluate the detector resolution. The tracking performance of a given layout is quantified by the resolution of the *track perigee parameters*, which are explained later on this section (Efficiencies and fake rates are not discussed in this work). The following cuts are applied on the truth particles in order to define the tracks that we are interested in reconstructing:

- $|\eta^{truth}| \leq 2.7$
- $|d_0^{truth}| < 1.0 \text{ mm}$
- $|z_0^{truth}| < 150 \text{ mm}$
- $p_0^{truth} > 1 \text{ GeV}$

This way we can now define what would be a reconstructed track. The track reconstruction cuts are:

- $|\eta^{truth}| \leq 2.7$
- $|d^{truth_0}| < 1.0$ mm
- $|z_0^{truth}| < 150$ mm
- $p_0^{truth} > 1$ GeV
- $N_{hits}^{si} \geq 9$
- $N_{holes}^{pix} = 0$

where $N_{hits}^{si} \geq 9$ stands for the total number of hits-on-track in all layers, and $N_{holes}^{pix} = 0$ for the number of Pixel layers traversed where a hit cannot be associated to a track.

The parameters that we are interested in are the longitudinal and transverse impact parameters, z_0 and d_0 . The d_0 parameter is defined as the distance from the point of closest approach A to the nominal interaction point P , whereas z_0 is the z coordinate of the point A . This parameters are illustrated in Figure 6. The resolution is obtained in the following way: The difference between the reconstructed and generated variable is computed for each event, the Root Mean Square (RMS) is calculated and a cut at $3RMS$ is applied, the resolution is taken as the σ of the cut.

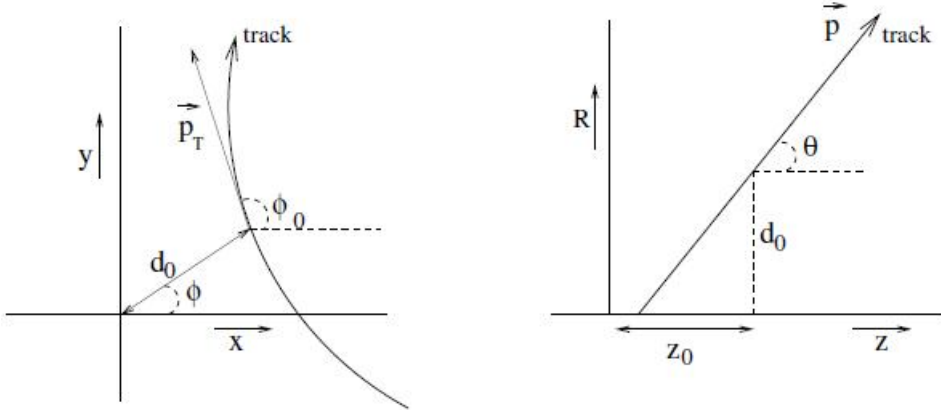


Figure 6: Illustration of the perigee Impact parameters of a track in the transverse plane (left) and rz -plane (right)

5 Results

In this section we present the comparison in the resolutions for the perigee parameter mentioned above when the simulated particles are muons. However before making any analysis on the resolutions we must verify that the simulated modules are actually working correctly. The pixel clusters on the rows and columns must show entries up to the following values if we are having a correct performance:

	50×250	50×50	100×100
Rows	672	672	336
Columns	240	1200	600

Table 3: Pixel clusters on the endcap Pixel detector for different values of the pixel size.

The values presented in Table 3 are obtained from the sensor dimensions and the pixel size in each sensor. It is important to mention that in order to cover the gaps between the sensors, bigger pixels are used in the perimeter of each sensor. The dimensions of these pixels are $450 \times 250 \mu m^2$ (for the three proposals), so we expect that these pixels receive more hits than the normal size pixels. The following plots illustrates what has been explained:

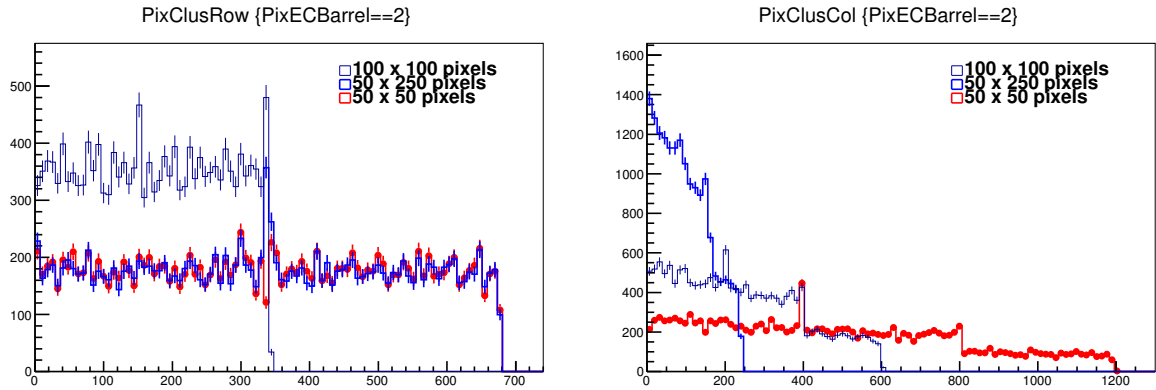


Figure 7: Plots showing the correct behavior of the simulated modules rows (left) and columns (right) in the endcap pixels

Now that we have verified the expected behavior of the simulated detector, we can proceed to do the resolution analysis. This is done for different p_T values : 5, 50 and 100 GeV . The d_0 and z_0 resolution for these values and for the different pixel sizes is compared in Figure 8

It is clearly seen that the resolution is much better for high values of p_T , regardless of the pixel size that is being used. Also, due to the order of magnitude in the resolution for low p_T , the improvement in the resolution is not significant. However if we “zoom

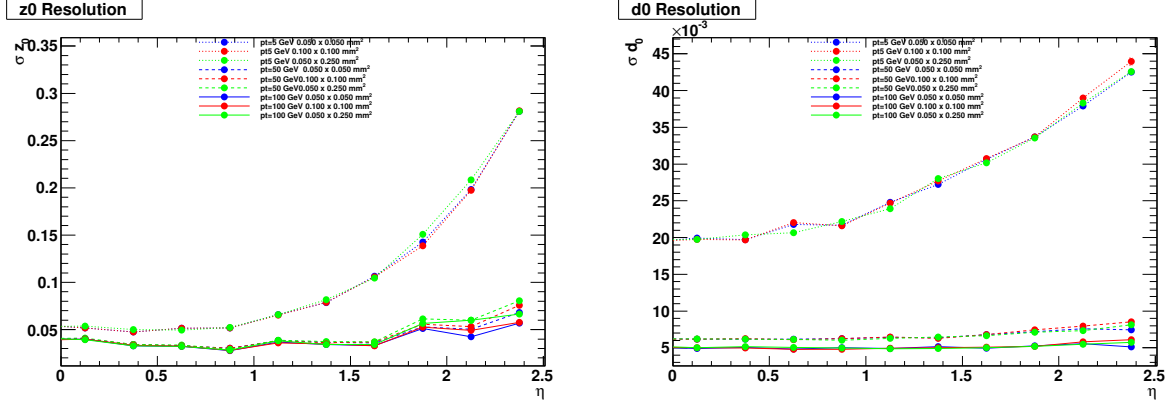


Figure 8: Resolution plots for the perigee impact parameters at different values of p_T .

in” to the resolutions for 100 GeV we can see that the resolution actually improves for the high granularity sensors (smaller pixel size):

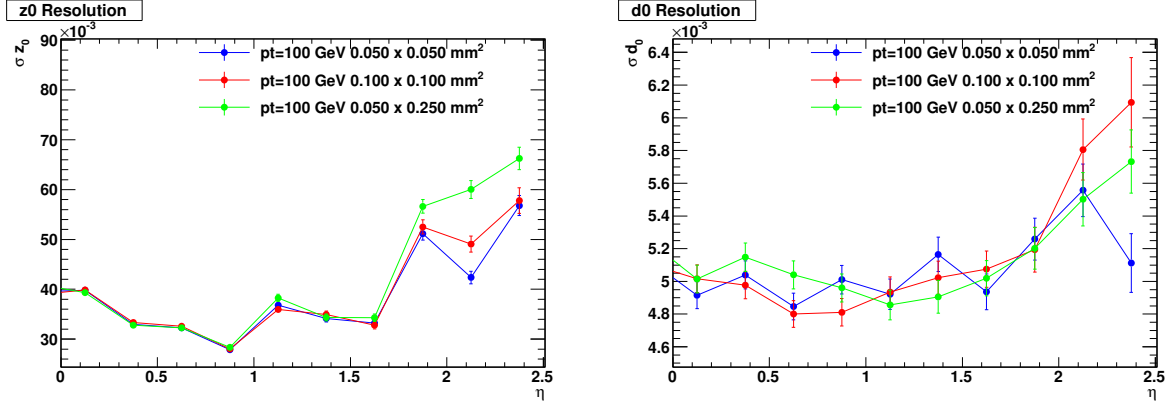


Figure 9: Resolution plots for the perigee impact parameters at $p_T = 100$ GeV.

6 Conclusions

An all-silicon using pixel and microstrip technology is the best option to overcome the difficulties that a high luminosity scenario presents. The desing of this detector is, however, still to be defined, and simulations have been carried out with three different proposals of the pixel size in the endcap disks ir order to evaluate which design offers the best resolution for the detector. The simulations show that the best resolution is obtained with the smallest pixel size, but this doesn't mean it is the best option since a balance between costs and benefits has to be considered. The next step is to make new design proposals (probably involving the pixel width) and to run simulations with high pile-up in order to obtain more precise results.

Acknowledgement

I would like to thank my supervisor, Nick, for all his support and patience for teaching me; to the Janet and Tiago for the very valuable ROOT lessons, and to Takanori for rescuing me when no one else was around. Special thanks to my professors in México: Arturo Fernández, Salvador Carrillo and Pedro Podesta, for their support and recommendations.

References

- [1] The ATLAS Collaboration, *Tracking Performance of the Proposed Inner Tracker Layout for the ATLAS Phase-II Upgrade*, ATLAS NOTE.
- [2] V. Vrba, *The ATLAS Pixel Detector*. Nuclear Instruments and Methods in Physics Research A 465 (2001) 27-33
- [3] ATLAS Computing Group, *Technical Design Report*. CERN-LHCC-2005-022
- [4] M. Garcia-Sciveres, *ATLAS Upgrades for High Luminosity*. Fermilab, July 7, 2009.